This article has been accepted for publication in a future issue of this journal, but has not been fully edited. Content may change prior to final publication. Citation information: DOI 10.1109/TIM.2019.2913612, IEEE Transactions on Instrumentation and Measurement

Non-Invasive Estimation of Plasma Sodium Concentration During Hemodialysis via Capacitively-Coupled Electrical Impedance Spectroscopy

Enrico Ravagli, Marco Crescentini, IEEE Member, Paolo Rovatti, and Stefano Severi*

***Abstract*— This paper presents a compact, low-cost, and non-invasive system for real-time estimation of plasma sodium concentration ($[Na]_{Pl}$) during a hemodialysis (HD) session with state-of-the-art accuracy. It is based on electrical impedance spectroscopy (EIS) performed with a capacitively-coupled impedance sensing cell and a high-frequency measurement device, both custom-built. The EIS data are processed to infer the resistance of the liquid inside the cell, which is used together with an optical hemoglobin sensor to estimate the $[Na]_{Pl}$. Validation of the EIS was performed by estimating the conductivity of blood-mimicking fluid (BMF). The complete method was validated using whole bovine blood, comparing the results to those obtained with standard instruments. The system was able to estimate the $[Na]_{Pl}$ with sufficient accuracy (RMS error of 3.0 mol/m^3 with respect to reference data) to provide clinically useful information. The proof-of-concept hardware can be converted to a cheap and compact circuit board for integration into an HD machine.**

***Index Terms*—Biomedical Measurement, Blood, Hemodialysis, Impedance Spectroscopy, Instrumentation, Sodium**

I. Introduction

A. Sensors in Hemodialysis

Chronic hemodialysis (HD) is a blood purification therapy for patients with little or no residual kidney functionality [1] [2]. Whereas some aspects of end-stage renal disease are treated pharmacologically, HD is required to perform the following: i) remove toxic byproducts of metabolism, ii) remove excess fluid, and iii) re-balance electrolytes. In a typical session, a vascular connection between the patient and the HD machine is established via a disposable hydraulic circuit, the *bloodline*. Blood passes through extracorporeal circulation, travels through a filter (the *dialyzer*), and returns to the patient. In the dialyzer, a sterile fluid (the *dialysate*), flows against the direction of blood flow, purifying the blood through diffusion and convection [3][4]. A diagram of this process is shown in Fig. 1.

Currently, several sensors are used in the HD machine for: operational control, safety, and monitoring of clinically relevant parameters. For example, optical or ultrasound sensors are used to estimate relative blood volume, starting from non-invasive measurements of hemoglobin concentration or total protein concentration [5]–[8]. Optical sensors have also been proposed to detect hemolysis [9] or improve the monitoring of filtration rate [10]. In another recently proposed solution, electrical measurements are used to detect blood leakage [11].

Monitoring plasma sodium concentration $[Na]_{Pl}$ would be particularly useful, since sodium is an osmotic regulator and a main driver for fluid shifts between the different body compartments [12][13]. Unfortunately, it cannot be measured non-invasively and repeatedly during the HD session. However, according to Kohlrausch's law of independent migration of ions in diluted electrolytic solutions [14], electrical conductivity is given by the sum of the specific ionic concentrations, weighted by ionic molar conductivity coefficients. Sodium concentration in plasma is the major

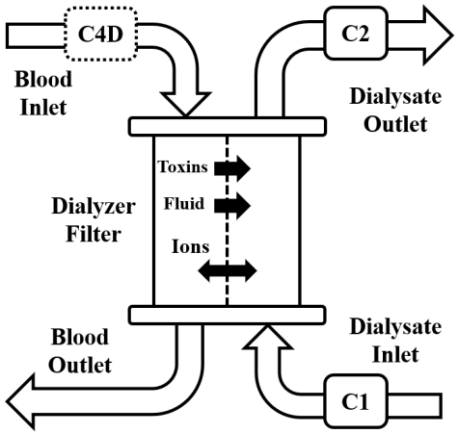

Fig. 1. Simplified diagram of the hemodialysis circuit. C1 and C2 are dialysate-side conductivity cells; C^{4}D is the non-invasive blood-side conductivity cell.

Manuscript received .....; revised .....; accepted ..... Date of publication .....; date of current version .....
Asterisk indicates corresponding author.

E. Ravagli was with the Department of Electrical, Electronic, and Information Engineering "Guglielmo Marconi", University of Bologna, Cesena, Italy. He is now with University College London.

M. Crescentini and S. Severi* (email: stefano.severi@unibo.it) are with the Department of Electrical, Electronic, and Information Engineering "Guglielmo Marconi", University of Bologna, Cesena, Italy.

Paolo Rovatti is with Baxter Research & Innovation, Gambro Dasco S.p.A., Medolla, Modena, Italy

DOI.....

This article has been accepted for publication in a future issue of this journal, but has not been fully edited. Content may change prior to final publication. Citation information: DOI 10.1109/TIM.2019.2913612, IEEE Transactions on Instrumentation and Measurement

contributor to plasma conductivity because it is one to two orders of magnitudes greater than the concentration of other ions, like potassium and calcium (140 mol/m^3 vs 10 mol/m^3 and 2 mol/m^3, respectively). Thus the electrical conductivity of plasma, (σ_{Pl}), which can be estimated [15], is correlated with $[Na]_{Pl}$. In fact, in HD, knowing σ_{Pl} has historically been considered as valid as knowing $[Na]_{Pl}$, due to their strong correlation [16].

The substitution of σ_{Pl} for $[Na]_{Pl}$ introduces uncertainty in the order of a few percentage points (depending on the exact concentration of the minority ions). However, the level of accuracy is sufficient to obtain clinical relevance in HD.

In addition to clinical knowledge, intra-session monitoring of σ_{Pl} and other variables with physiological significance plays a role in biofeedback systems [17]–[23] and facilitates customizing the therapy for each patient.

The step-based protocol developed by Polaschegg [15], which is the state-of-the-art technique for σ_{Pl} estimation, relies on two conductivity cells placed upstream and downstream from the dialyzer (see C1 and C2 in Fig. 1). However, it is not very accurate, requires ≃10 minutes for a single measurement, and can only be repeated a few times in a session. Recently, a new, non-invasive method to estimate the conductivity of liquids in a bloodline was reported by our group [24], which has the potential to be faster and more accurate than the state-of-the-art. This achievement (described in more detail in Section I.B) is expanded upon by developing compact low-cost hardware and a model for estimating $[Na]_{Pl}$ from the blood impedance.

B. Non-invasive conductivity estimation in Hemodialysis

In [24], a capacitively-coupled contactless conductivity detection (C^{4}D) cell developed by our group for the non-invasive estimation of electrical conductivity of liquids is described. In C^{4}D, two ring electrodes are placed externally around a liquid-filled tubing segment. When a high-frequency stimulation signal is applied, electrode-tubing-liquid interfaces act as series capacitors and current is capacitively coupled through the liquid (which acts as a resistor). The high-frequency impedance is related to the resistance (and so, to the conductivity) of the liquid [25][26].

This technology was adapted to HD, by i) creating a C^{4}D cell specific for HD, ii) performing electrical impedance spectroscopy (EIS) at high frequency with a professional impedance analyzer, and iii) characterizing the electrode-bloodline interaction with an electrical model based on the constant phase element (CPE) [27-30].

The previously developed C^{4}D cell consists of two cylindrical aluminum electrodes of length 20 mm placed at 70 mm (center-to-center) from each other. The electrodes are round-shaped, 10-mm wide, with internal diameter of 6 mm. Electrodes are contained in an aluminum electromagnetic shielding box and connected to the external environment with simple copper wiring and screw connectors. The cell was designed to host a specific type of polymeric biocompatible line used for hemodialysis treatment (ArtiSet blood tubing system, Baxter, Medolla, Italy) with an external diameter of 6.5 mm and an internal diameter of 4 mm.

The proposed location of the cell in the HD hydraulic circuit is shown in Fig. 1. Fig. 2 shows a simplified representation of the complete system, which allowed to estimate the conductivity of a saline solution and of a blood-mimicking fluid (BMF). The estimate is sufficiently accurate to be clinically useful in HD, without the many disadvantages of the state-of-the-art method.

C. Scope of this work and organization of the paper

This work describes a compact, low-cost system for the non-invasive estimation of plasma sodium concentration during HD. The rationale is that whole blood conductivity, measured by the C^{4}D cell, can be used for accurate estimation of plasma sodium. The system is shown to be sufficiently accurate for clinical relevance, and suitable for integration into an HD machine. This paper describes the hardware design of the electronic system that can replace the professional impedance analyzer, as well as the measurement process which estimates the plasma concentration from the impedance data. The hardware and the measurement procedure are described in Section II; experimental results are reported and commented on in Section III. Final discussions are developed in Section IV.

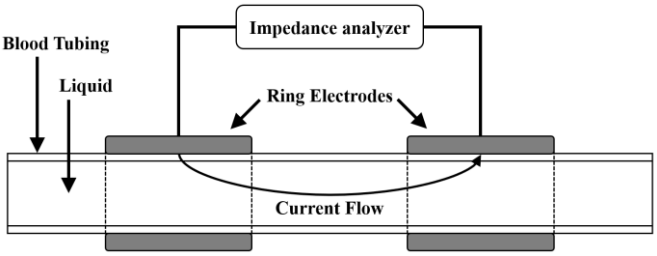

Fig. 2. Simplified representation of our non-invasive C^{4}D cell for hemodialysis.

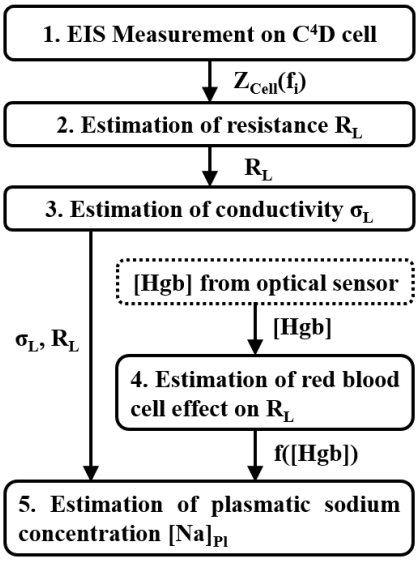

Fig. 3. Steps of the proposed $[Na]_{Pl}$ estimation method.

This article has been accepted for publication in a future issue of this journal, but has not been fully edited. Content may change prior to final publication. Citation information: DOI 10.1109/TIM.2019.2913612, IEEE Transactions on Instrumentation and Measurement

II. METHODS

In Fig. 3, a diagram of the proposed $[Na]_{Pl}$ estimation methodology is shown. In Step #1, Electrical Impedance Spectroscopy (EIS) is performed on the C^4D-based sensing cell. A compact and low-cost hardware solution, fit for integration into an HD machine, was developed for this purpose. Subsection II.A gives the details of our EIS hardware architecture together with the mathematical and software operations required to obtain valid results. In Step #2, the resistance R_L of the liquid contained into the cell is determined (starting from the EIS data) by means of mathematical modelling. This procedure is described in Subsection II.B. In Step #3, the conductivity σ_L of the liquid (in this case, whole blood) is estimated from R_L by means of linear regression. This step is described in Subsection II.C. Step #3 serves primarily as a comparison with the previous work [24], since σ_L despite being part of the theoretical process for estimation of $[Na]_{Pl}$ is not part of the final equation. Step #4 compensates for the effect on R_L of the presence of red blood cells (RBCs) in whole blood by estimating the hemoglobin concentration in blood ([Hgb]) with an optical sensor commonly present on HD machines. This process is reported in Subsection II.D. In Step #5, $[Na]_{Pl}$ is estimated.

A. Hardware Architecture and EIS Measurement

A compact, low-cost electronic system, capable of being combined with an HD machine, was developed to perform EIS. The system's goal was the non-trivial task of measuring complex impedances in the order of tens of kΩ in the MHz range. A conceptual diagram of the EIS system, and an image of the implemented prototype, which is ≃20x10x10 cm in size, are shown in Fig. 4.

The system operates by applying a sinusoidal voltage V_{Stim} to the impedance under analysis (i.e. the C^4D cell), and picking up a sensing current I_{Sens} (which is converted to voltage V_{Sens}). A high-speed data acquisition board digitizes both V_{Stim} and V_{Sens}, and a 3-parameter sine-fitting procedure is performed to estimate their amplitude, phase, and DC offset. The complex impedance is then computed from the amplitude ratio and phase difference for the two signals.

A custom-designed printed circuit board (PCB) generates and processes the analog signals. V_{Stim} is generated by a discrete digital synthesis (DDS) module based on the AD9850 (Analog Devices, Norwood, USA). This signal is pre-processed to increase the amplitude and remove DC offset by means of operational amplifier-based filter and gain stages. The nominal V_{Stim} amplitude is 2 V. The current I_{Sens} is picked up from the ring electrodes, filtered, and amplified by a current-to-voltage converter, resulting in the V_{Sens} signal. For all the analog stages, the AD8066 operational amplifier was chosen due to its high bandwidth and input impedance.

An Arduino Uno microcontroller-based prototyping board is used to program the DDS module in order to output different frequencies. For each frequency, the Arduino system programs the DDS through a serial protocol (Frequency Programming in Fig. 4a) and commands the recording of sine wave data by means of a digital pin used as flag, which is raised when all the transients are concluded (Frequency Information in Fig. 4a).

A frequency range of 1–1.5 MHz was chosen. The minimum frequency allows significant coupling of current through the capacitive electrodes; that is, the series impedances are sufficiently low to allow the detection of impedance variations in blood. A maximum frequency of 1.5 MHz provides a sufficiently wide frequency span for robust regression of EIS data, while maintaining a low enough frequency that part of the current is still confined to plasma. EIS measurements were performed at six frequencies, covering the 1–1.5 MHz range in 100-kHz steps.

A ProLogic16 FPGA-based data acquisition board (Salae, San Francisco, USA) was chosen to record V_{Stim} and V_{Sens}. The recording process starts on the rising edge of the flag pin; thus, it is asynchronous with respect to the generation of the stimulus signal. The two sine waves V_{Stim} and V_{Sens} are sampled at 50 MHz, with a channel-to-channel skew of less than 1 sample. Each recording session lasts 20 ms (limited by the memory of the ProLogic board), leading to the recording of more than 20000 sine periods per signal.

A compact power converter (TML20205C, Traco Power, Baar, Switzerland) supplies dual ±5 V voltage to the PCB and 5 V to the Arduino system. A custom 3D-printed housing holds all the electronics modules together. The entire

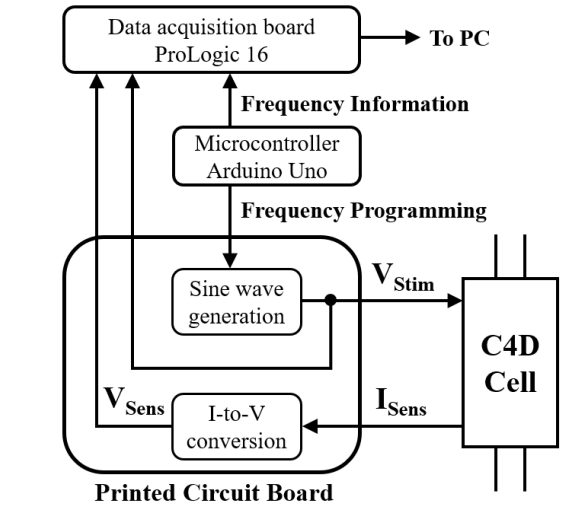

(a)

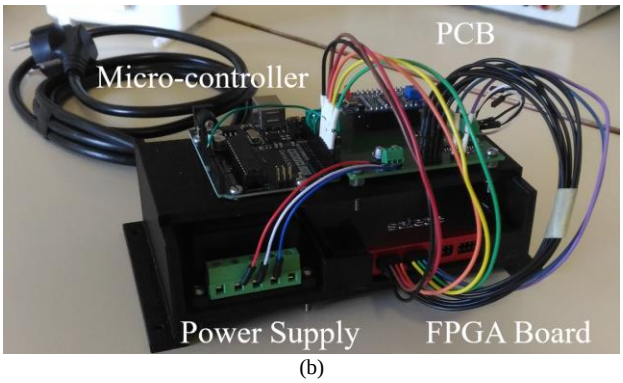

(b)

Fig. 4. (a) Conceptual diagram of the EIS measurement system. (b) Image of the real-world prototype.

This article has been accepted for publication in a future issue of this journal, but has not been fully edited. Content may change prior to final publication. Citation information: DOI 10.1109/TIM.2019.2913612, IEEE Transactions on Instrumentation and Measurement

prototype (Fig. 4b) was placed inside a grounded aluminum box (not shown) for electromagnetic shielding.

Data recorded from the ProLogic board were exported and processed using Matlab for the sake of simplicity, but future data processing could be performed directly on the microcontroller unit. For each frequency f_i, V_{Stim} and V_{Sens} were fitted to the following equations:

$$V_{Stim,i}(t) = C_{0,i} + A_{0,i} \cdot \sin\left(2\pi f_i t + \varphi_{0,i}\right), \quad i = 1..6 \quad (1)$$
$$V_{Sens,i}(t) = C_{1,i} + A_{1,i} \cdot \sin\left(2\pi f_i t + \varphi_{1,i}\right), \quad i = 1...6 \quad (2)$$

A set of three parameters (C, A, φ) was obtained for each of the two signals and each of the six frequencies by sine fitting, according to the IEEE-1057 standard [31]. Despite not performing any proper averaging, the application of the sine fitting algorithm over the very large number of recorded sine periods considerably reduces the effect of additive random noise on the parameter estimation. Afterwards, the magnitude and phase of the C^{4}D cell's impedance Z_{Cell} were computed:

$$\left|Z_{Cell,i}\right| = \frac{A_{0,i}}{A_{1,i}} \cdot \frac{1}{G_{Comp}(f_i)} \quad (3)$$
$$arg\left(Z_{Cell,i}\right) = \varphi_{0,i} - \varphi_{1,i} - \varphi_{Comp}(f_i), \quad (4)$$

The compensation factors G_{Comp} and φ_{Comp} were applied to correct for the (previously characterized) gain and phase responses of the custom PCB board, and for the channel-to-channel skew of the ProLogic data acquisition board. Real (R) and imaginary (X) parts of the impedance were then computed:

$$R_i = \left|Z_{Cell,i}\right| \cdot \cos\left(arg\left(Z_{Cell,i}\right)\right) \quad (5)$$
$$X_i = \left|Z_{Cell,i}\right| \cdot \sin\left(arg\left(Z_{Cell,i}\right)\right) \quad (6)$$

B. Impedance modeling

As discussed in the previous work [24], the CPE is a good model of the electrical coupling between the electrodes and the bloodline's polymer. Our group recently confirmed the presence of the CPE effect in electrode-polymer coupling for bloodlines from several different manufacturers [32], showing it is a common feature of the bloodlines. When a liquid is far away from the electrode-liquid interface, it is usually modelled as a resistance. Thus, the lumped parameters electrical model of the C^{4}D cell at frequency f_i is composed of the series connection of a CPE element and R_L, the resistance of the liquid which fills the segment of bloodline between the electrodes. This model is shown in Eq. (7), where K_{CPE} and α_{CPE} are the CPE element parameters.

$$Z_{Cell,i} = R_L + \frac{K_{CPE}}{(j2\pi f_i)^{\alpha_{CPE}}} \quad (7)$$

To estimate R_L, the EIS data from Subsection II.A could be fitted to Eq. (7); however, that would be an iterative process. For this specific electrical model, it is much easier to estimate R_L by considering that for $f\to\infty$, $Z_{Cell}\to R_L$, meaning that Z_{Cell} will cross the real axis of the complex plane exactly at R_L. The intercept for $Z_{Cell}(f\to\infty)$ on the real axis is easily found by performing a linear regression on the EIS data in the complex plane. This least-squares fitting process is faster than the iterative method.

C. Conductivity Estimation

According to Ohm's second law, the conductivity of the liquid, σ_L, is directly proportional to the reciprocal of the liquid's resistance R_L, i.e. its admittance G_L. Specifically, σ_L and G_L are related by a parameter representing the geometrical shape factor of the current path. In our case, this constant is related to the length and lumen area of the bloodline segment between the cell's electrodes.

D. Plasma Sodium Estimation

The resistance R_L of whole blood is related to its conductivity σ_{Bl}:

$$R_L = \frac{1}{\sigma_{Bl}} \cdot \frac{l}{S} \quad (8)$$

where l and S are the length and internal section area of the bloodline segment inside the C^{4}D cell, respectively. As explained in I.A, $[Na]_{Pl}$ strongly correlates with plasma conductivity σ_{Pl} [16]. For the purpose of this work, a direct linear relationship between σ_{Pl} and $[Na]_{Pl}$ was assumed, without an offset term but with a fixed proportionality coefficient, C_{Na}, expressed in [S·m^2·mol^{-1}]:

$$\sigma_{Pl} = C_{Na} \cdot [Na]_{Pl} \quad (9)$$

To relate σ_{Bl} to σ_{Pl}, the mathematical model needs to account for the effect of RBCs on conductivity. Fortunately, the relationship between the composition of whole blood and its electrical properties has been extensively studied in the last few decades [33]-[38]: briefly, at sufficiently low frequencies, the β dispersion (the electrical coupling across the RBC membranes [38][39]) is negligible, and the electrical current only passes through the plasma. In this case, σ_{Bl} can be modeled as a fraction of σ_{Pl}:

$$\sigma_{BL} = \sigma_{Pl} \cdot f([Hgb]) \quad (10)$$

with an attenuation factor to model the occluding effect of the RBCs. Although this factor is usually a function of hematocrit (Hct) [35]–[37], [Hgb] was chosen instead, since this information is readily available in HD from optical sensors [5]. For f([Hgb]) an exponential model was chosen:

$$f([Hgb]) = e^{-\frac{[Hgb]}{\tau_{Hgb}}} \quad (11)$$

The model is physically sound, since for [Hgb]=0 it gives $\sigma_{Bl}=\sigma_{Pl}$ (current flows freely), and for $[Hgb]\to\infty$, $\sigma_{Bl}=0$ (current is completely blocked). A more detailed analysis of the behaviour of this model as it approaches asymptotical values of [Hgb] has no practical meaning, since [Hgb] is

This article has been accepted for publication in a future issue of this journal, but has not been fully edited. Content may change prior to final publication. Citation information: DOI 10.1109/TIM.2019.2913612, IEEE Transactions on Instrumentation and Measurement

regulated by pathophysiology and extreme values are incompatible with life.

Eqs. (8–11) can be put together and all the fixed parameters except for τ_{Hgb} can be grouped into –a single parameter C_{Tot}, as shown in Eq. (12), which is used in Step #5 of the estimation process.

$$[Na]_{Pl} = \frac{1}{R_L} \cdot \frac{1}{f([Hgb])} \cdot \left(\frac{l}{S} \cdot \frac{1}{C_{Na}}\right) = \frac{1}{R_L} \cdot \frac{1}{f([Hgb])} \cdot C_{Tot} \quad (12)$$

Although conductivity is conceptually part of the estimation process, practically speaking only R_L and [Hgb] are needed to estimate $[Na]_{Pl}$. Values of C_{Tot} and τ_{Hgb} were fitted from experimental data.

III. Experimental Results

A. EIS Measurements and estimation of BMF conductivity

Preliminary experimental validation of our system was performed on blood-mimicking fluid (BMF), which is considered as a simple yet representative fluid. Fig. 5 shows an example of sine-fitting results from BMF data at f=1 MHz for both stimulation and sensing signals. Typical root-mean-square-errors (RMSE) of the fitting process are 39 mv (R^2=0.9996) for the stimulation signal, which has a nominal amplitude of 2 V (see Fig. 5a), and 5.5 μA (R^2=0.9947) for the sensing signal, which is in the order of magnitude of 80 μA (see Fig 5b).

Five samples of BMF composed of 20% Intralipid (Fresenius Kabi Italia Srl, Isola della Scala, Italy) and different amounts of NaCl were prepared. Conductivities of the BMF samples were set to whole blood physiological levels (5-10 mS/cm) [33][34][40]. The presence of lipid corpuscles in Intralipid mimic the presence of RBCs in the blood. Reference conductivities $\sigma_{BMF,Ref}$ were measured before the experiments using a lab conductivity meter (EDGE, Hanna Instruments, Padova, Italy; accuracy class ±1 %). EIS measurements were performed at room temperature by injecting the fluid samples into a piece of HD polymeric line placed in the measurement cell.

Samples were injected in order of increasing and then decreasing conductivity, for a total of ten measurements. In between measurements, the line was washed with ultrapure water. Fig. 6 illustrates the EIS data collected. For a cleaner representation, only data from the first five EIS measurements are shown (that is, corresponding to ascending conductivity).

Reference conductivity values of the five samples were 5.16, 6.14, 7.27, 8.38, 9.95 mS/cm. It is clear from Fig. 6 that EIS measurements on BMF show the same CPE coupling effect reported previously [24]. The figure's dashed lines show the linear regressions that allow the estimations of R_{BMF} and, consequently, G_{BMF}.

Fig. 7 shows the correlation between $\sigma_{BMF,Ref}$ and $\sigma_{BMF,Est}$, the latter computed from admittance G_{BMF} by linear regression through eq. (8) (R^2 = 0.98). The RMSE between estimated and reference conductivity was 0.24 mS/cm.

B. Estimation of plasma sodium in whole blood

The second stage of validation was performed on whole blood. Experiments were performed in compliance with all national regulations, using fresh anticoagulated bovine blood. During each experimental session, the blood was magnetically stirred in a glass container at room temperature. The blood's relevant physiological parameters ([Hgb], Hct, $[Na]_{Pl}$ and osmolarity) were varied by means of dilution with ultrapure water, dilution with sodium chloride (NaCl) solutions at various concentrations, and direct dissolution of NaCl in blood. All the sample points are within pathophysiological ranges: 134-169 mol/m^3 for $[Na]_{Pl}$ and 5.5–15.1 g/dL for

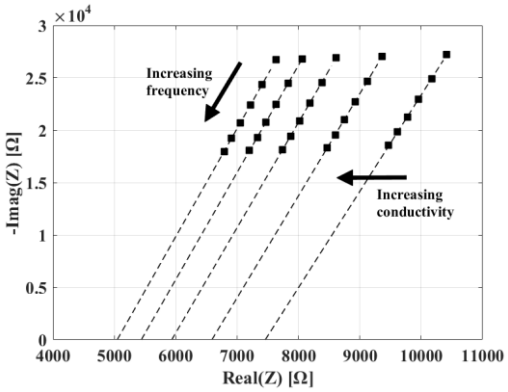

Fig. 6. EIS experimental data (black dots) for each of the five BMF samples. Linear regression for each EIS spectrum is shown in dashed line.

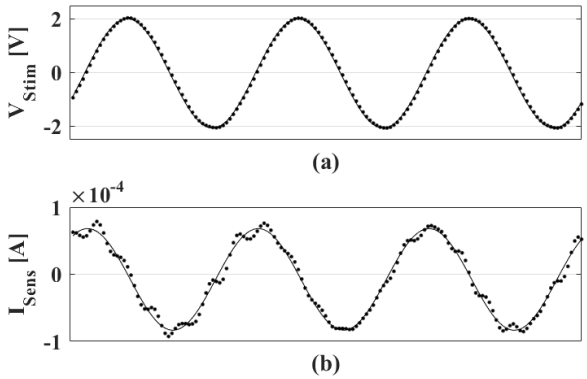

Fig. 5. Example of sampled data (dots) and its least-squares fitting (line) for (a) stimulation voltage V_{Stim} and (b) pick-up current I_{Sens}.

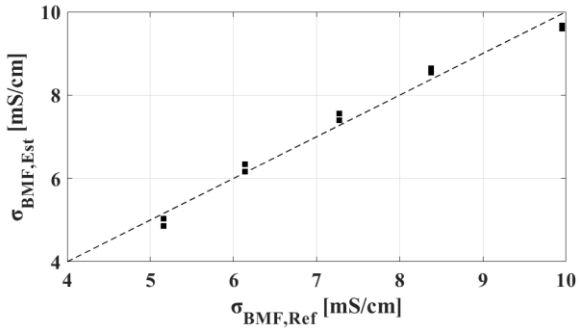

Fig. 7. Comparison of reference and estimated conductivity of blood mimicking fluid, shown in black squared. Dashed line shows identity i.e. $\sigma_{BMF,Est}$=$\sigma_{BMF,Ref}$.

This article has been accepted for publication in a future issue of this journal, but has not been fully edited. Content may change prior to final publication. Citation information: DOI 10.1109/TIM.2019.2913612, IEEE Transactions on Instrumentation and Measurement

[Hgb].

A total of N=27 sample points were collected from five experimental sessions. Fig. 8 illustrates the distribution of the collected sample points in the [Na]/[Hgb] space and shows that our dataset samples cover a relevant and meaningful subset of the pathophysiological [Na]/[Hgb] space. After applying each modification to blood composition, a wait time was imposed to allow mixing and the reference [Hgb] was measured with an optical instrument (Hb301, HemoCue, Ängelholm, Sweden, uncertainty assessed at 0.7 g/dL [41]). The Hct, $[Na]_{Pl}$ and osmolarity were measured using an emergency-room-grade blood-gas analyzer (i15, Edan Instruments, Shenzen, China, sodium concentration uncertainty assessed to 1.6 mol/m^3). The EIS measurements were performed at the same time as these reference measurements. A segment of HD bloodline (ArtiSet blood tubing system, Gambro Spa, now part of Baxter, USA) had been placed inside the C^{4}D sensing cell before the start of the experiment. The cell was filled with blood, clamped at the ends and the EIS measurement was performed within seconds. The bloodline was washed after each measurement to avoid contamination.

For the whole dataset, the correlations for [Hgb]/Hct and [Na]/osmolarity were high (R^2=0.94 and R^2=0.98, respectively). These results demonstrate that no significant error was introduced by: i) choosing [Hgb] over Hct or ii) modeling the relationship between sodium and osmolarity as linear.

The fitting of experimental data for estimation of parameters C_{Tot} and τ_{Hgb} (and subsequently estimation of $[Na]_{Pl}$) were first estimated by performing a fitting process on the whole dataset (best case). The process was then repeated using a leave-one-out procedure to get a more realistic error quantification.

For the whole dataset, the fitting process returned parametric values of C_{Tot}=7.02e^5±0.11e^5 mol·m^{-3}·S^{-1} and τ_{Hgb}=36.4±1.8 g/dL. A visual representation of the best fit is shown in Fig. 9.

The estimation of $[Na]_{Pl}$ using parameters C_{Tot} and τ_{Hgb} computed from the whole dataset returned an RMSE of 3.0 mol/m^3. The correlation factor between $[Na]_{Pl,Est}$ and $[Na]_{Pl,Ref}$ was R^2=0.90. Estimation using a leave-one-out procedure returned an RMSE of 3.3 mol/m^3 (R^2=0.88). In Fig. 10, the relationship between estimated and experimental $[Na]_{Pl}$ values is shown.

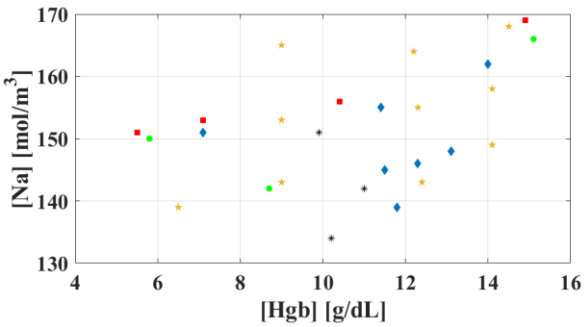

Fig. 8. Maps of the dataset sample points. This is a visual representation of how the collected sample points are distributed over the pathophysiological population space in the [Na]/[Hgb] domain. Different colors and symbols represent data collected during a different session.

IV. Discussion

A. Results

The authors' work established that estimation of BMF conductivity is possible using a C^{4}D cell and a professional impedance analyzer, and also quantified the estimation RMSE as 0.06 mS/cm with respect to reference data. In the present work, BMF conductivity was again estimated, using the same cell, but the impedance analyzer was replaced with a compact, low-cost device. The estimation returned an RMSE of 0.24 mS/cm, a 4-fold increment. However, the proposed device could be as much as 100 times cheaper than the commercial instrument. This advantage, particularly when considered together with the fact that 0.24 mS/cm is still a clinically acceptable accuracy level for conductivity, constitutes an excellent intermediate result for our system.

A major novelty of the present work is the estimation of plasma sodium. The validation of the device plus the estimation model on whole blood returned an RMSE of 3.0 mol/m^3. This amount of scatter is in line with the accuracy of blood gas analyzers [42], indicating that this new system is almost as accurate as the reference instrument and that the estimation model is theoretically correct. Moreover, although the most important source of uncertainty, the presence of other ions, cannot be eliminated with the proposed method, it can be assessed to a few percentage points. Clearly, the final accuracy

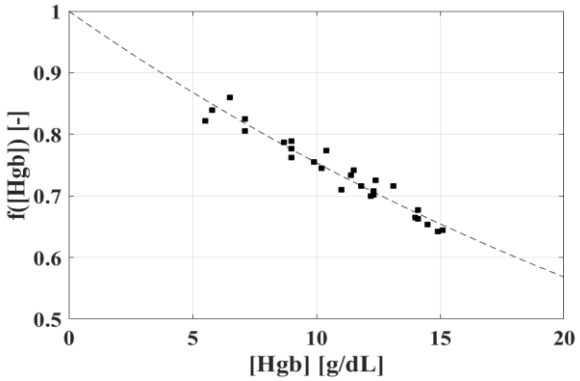

Fig. 9. Fitting of [Hgb] data to the model reported in eq. (11). Black squares represent experimental data, black dashed line is the best-fit model.

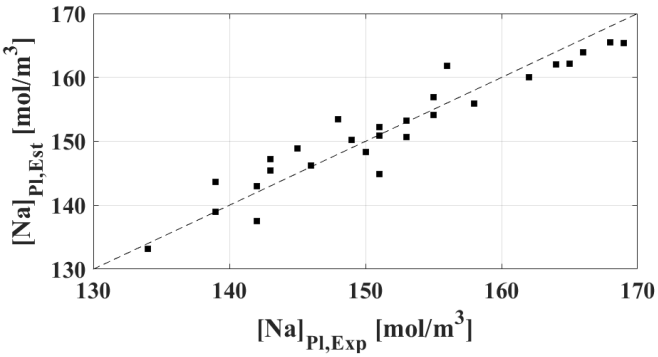

Fig. 10. Estimated vs. experimental [Na] values. Black dots represent points from the dataset. Black dashed line is the ideal relationship, i.e. identity.

This article has been accepted for publication in a future issue of this journal, but has not been fully edited. Content may change prior to final publication. Citation information: DOI 10.1109/TIM.2019.2913612, IEEE Transactions on Instrumentation and Measurement

is sufficient for HD systems, since cost and physical dimension also play important roles.

An additional source of uncertainty is the lab bench instrument providing the optical measurement which quantified the effect of [Hgb]: its accuracy was quantified as 0.7 g/dl. In future developments, this instrument will be replaced with less-accurate integrated optical sensors embedded in HD machines, like the Hemoscan [5].

The estimation error computed using a leave-one-out procedure on the data was only slightly larger than that computed with parameters estimated on the whole dataset, indicating that the parametric values are robust and that the system is feasible for real applications.

Thus, results indicate that the developed system is a valid solution for the non-invasive estimation of plasma sodium concentration of whole blood in HD bloodlines. A practical and potentially very useful application the system could be the implementation of a real isonatric dialysis therapy, that has been recently shown to improve the blood pressure control in HD patients [43].

B. Technical aspects

Regarding the geometrical parameters of the previously developed C^4D cell, modification of such parameters could allow for improved sensitivity. For example, increasing the length of the electrodes would increase coupling surface and thus lower coupling impedance; increasing distance of the electrodes would increase the weight of the liquid's resistance on the total measured impedance, thus increasing sensitivity. Thus, larger and more distant electrodes could help increase sensitivity; however, such modifications would make the cell too large for real-life applications. The current cell was designed with a choice of geometry which allows satisfying measurements while keeping the volume compatible with practical use on an HD machine. Another factor of influence is the bloodline: thickness and material will influence the magnitude and phase of the CPE coupling effect similarly to how thickness and dielectric constant affect the capacitance in a cylindrical capacitor. However due to de-facto standards, most bloodlines will have similar thickness and composition; electrical properties of bloodlines from different brands are analyzed in [32].

The system was built using a relatively simple hardware architecture: a commercial data acquisition board, a microcontroller, and a small custom PCB. However, volume and cost could be reduced even further. A single dedicated PCB, approximately 20x10cm, would be quite economical and could contain all the necessary components. The board could also work in real time, and the number of frequencies and sine periods recorded for the estimate could be reduced for faster sampling.

In order to estimate [Hgb], the system requires information from an optical sensor. Although this technically means relying on an external source of data, optical [Hgb] sensors are commonly embedded in HD machines and thus they will be part of the final application for our method.

In Section II.D, the electrical behavior of blood is modeled as purely resistive, meaning that all current is assumed to flow in the plasma. This assumption is valid up to the occurrence of β dispersion, reported to be in the range of 1–100 MHz [38]. Due to the constraints mentioned above, the operational frequency range chosen for this work (1–1.5MHz) falls right at the onset of this phenomenon. However, our frequency span is only bordering on the β dispersion region, and the current flowing inside RBCs can still be assumed to be negligible. The satisfactory results obtained in fitting experimental data and estimating sodium concentration demonstrate the validity of this assumption, and, consequently, of the impedance model.

C. Limitations and Future Developments

In order to test the developed system in a tightly controlled experimental setup, measurements were performed on segments of bloodline with both ends isolated by mechanical clamps, without fluid flow. Further, [Hgb] data were obtained from an optical sensor other than the one embedded in an HD machine, although it is very similar in architecture. The blood gas analyzer used for reference sodium concentration measurements was not particularly accurate, but it was appropriate in this preliminary phase for its fast response time.

Although the proposed technique shows promising results for determining plasma sodium concentration into a bloodline, further work is required to provide evidence that this system is validated for application during HD, when blood flows through the bloodline.

In the future, the system will be tested on an experimental setup which includes a state-of-the-art HD machine and a complete hydraulic circuit with flowing blood. The optical [Hgb] measurements will be performed by the HD machine, and the resulting data will be plugged into the estimation algorithm. More accurate reference blood sodium concentration measurements will also be performed by means of chemical lab analyses.

V. Conclusion

The use of electrical impedance spectroscopy with a sensing cell based on non-invasive signal coupling is a promising method for the estimation of plasma sodium concentration during HD. Additional data (e.g. from an optical sensor) is required to correct for the effect of the erythrocytes on the total conductivity of blood. Significantly, the proof-of-concept hardware presented in this work can be easily converted to a cheap and compact printed circuit board ready for integration into an HD machine. The method described here, though requiring validation in clinical conditions, has the potential for very fast, almost continuous, sodium estimation, which would be a novel and important improvement on current HD machines. The ability to monitor plasma sodium concentration in real time throughout the HD session would allow for better biofeedback algorithms, and, as a consequence, will also improve patient health.

Acknowledgment

E. R. PhD studentship was funded by Gambro-Dasco (now part of Baxter). The authors would like to thank Maurizio

Lannocca for his help in developing the measurement system and Mariano Ruffo for his support during the experiments, and Kristina Mayberry for language revision.

REFERENCES

[1] A. M. Davison, *Oxford Textbook of Clinical Nephrology Volume 3*. Oxford University Press, 2005.

[2] A. Nissenson and R. N. Fine, *Clinical Dialysis, Fourth Edition*. McGraw Hill Professional, 2005.

[3] J. A. Sargent and Gotch F.A., "Principles and biophysics of dialysis," in *Replacement of Renal Function by Dialysis*, Springer., W. Drukker, F.M. Parsons, J.F. Maher, 1983.

[4] C. Ronco *et al.*, "The haemodialysis system: basic mechanisms of water and solute transport in extracorporeal renal replacement therapies," *Nephrol. Dial. Transplant.*, vol. 13 Suppl 6, pp. 3–9, 1998.

[5] F. Paolini *et al.*, "Hemoscan: a dialysis machine-integrated blood volume monitor," *Int J Artif Organs*, vol. 18, no. 9, pp. 487–494, Sep. 1995.

[6] J. J. Dasselaar *et al.*, "Relative blood volume measurements during hemodialysis: comparisons between three noninvasive devices," *Hemodial Int*, vol. 11, no. 4, pp. 448–455, Oct. 2007.

[7] I. Yoshida *et al.*, "A new device to monitor blood volume in hemodialysis patients," *Ther Apher Dial*, vol. 14, no. 6, pp. 560–565, Dec. 2010.

[8] E. Mancini *et al.*, "Intra-dialytic blood oxygen saturation (SO2): association with dialysis hypotension (the SOGLIA Study)," *J. Nephrol.*, vol. 30, no. 6, pp. 811–819, Dec. 2017.

[9] S. Cattini and L. Rovati, "An Optical Technique for Real-Time Monitoring of Hemolysis During Hemodialysis," *IEEE Trans Instrum Meas*, vol. 65, no. 5, pp. 1060–1069, May 2016.

[10] A. Visotti *et al.*, "A Differential Optical Sensor for Non-Invasive Real-Time Monitoring of Ultrafiltration Rate in Hemofiltration Therapies," *IEEE Sensors J*, vol. 18, no. 20, pp. 8597–8604, Oct. 2018.

[11] P. Huang *et al.*, "Integration of wireless flexible sensor and virtual internal impedance model for blood leakage detection during haemodialysis," *IET SCI MEAS TECHNOL*, vol. 12, no. 5, pp. 617–625, 2018.

[12] M. J. Flanigan, "Role of sodium in hemodialysis," *Kidney Int. Suppl.*, vol. 76, pp. S72-78, Aug. 2000.

[13] Heineken F. G. *et al.*, "Intercompartmental Fluid Shifts in Hemodialysis Patients," *BIOTECHNOL PROGR*, vol. 3, no. 2, pp. 69–73, Sep. 2008.

[14] R. A. Robinson and R. H. Stokes, *Electrolyte Solutions: Second Revised Edition*. Dover Publications, Incorporated, 2012.

[15] H. D. Polaschegg, "Automatic, noninvasive intradialytic clearance measurement.," *Int J Artif Organs*, vol. 16, no. 4, pp. 185–191, Apr. 1993.

[16] F. Locatelli, S. Di Filippo, and C. Manzoni, "Relevance of the conductivity kinetic model in the control of sodium pool," *Kidney Int. Suppl.*, vol. 76, pp. S89-95, Aug. 2000.

[17] S. Stiller *et al.*, "A critical review of sodium profiling for hemodialysis," *Semin Dial*, vol. 14, no. 5, pp. 337–347, Oct. 2001.

[18] A. Santoro *et al.*, "Blood volume controlled hemodialysis in hypotension-prone patients: a randomized, multicenter controlled trial," *Kidney Int.*, vol. 62, no. 3, pp. 1034–1045, Sep. 2002.

[19] S. Cavalcanti *et al.*, "Model-based study of the effects of the hemodialysis technique on the compensatory response to hypovolemia," *Kidney Int.*, vol. 65, no. 4, pp. 1499–1510, Apr. 2004.

[20] F. Locatelli *et al.*, "Haemodialysis with on-line monitoring equipment: tools or toys?," *Nephrol. Dial. Transplant.*, vol. 20, no. 1, pp. 22–33, Jan. 2005.

[21] S. Severi *et al.*, "Cardiac response to hemodialysis with different cardiovascular tolerance: heart rate variability and QT interval analysis," *Hemodial Int*, vol. 10, no. 3, pp. 287–293, Jul. 2006.

[22] J. J. Dasselaar, "Relative blood volume based biofeedback during haemodialysis," *J Ren Care*, vol. 33, no. 2, pp. 59–65, Jun. 2007.

[23] A. Santoro, E. Mancini, and A. T. Azar, "Biofeedback Systems and Their Application in the Hemodialysis Therapy," in *Modeling and Control of Dialysis Systems*, Springer, Berlin, Heidelberg, 2013, pp. 1081–1107.

[24] E. Ravagli *et al.*, "Non-invasive measurement of electrical conductivity of liquids in biocompatible polymeric lines for hemodialysis applications," *Sens Actuators A Phys*, vol. 261, no. Supplement C, pp. 252–260, Jul. 2017.

[25] M. Crescentini, M. Bennati, and M. Tartagni, "Design of integrated conductivity-temperature-depth (CTD) sensors", AUE Int J electronics and Comm, vol. 66, no. 8, pp. 630-635, 2012.

[26] M. Crescentini, M. Bennati, and M. Tartagni, "A High Resolution Interface for Kelvin Impedance Sensing", *IEEE J Solid State Circ*, vol. 49, no. 10, pp. 2199-2212, Oct 2014.

[27] G. J. Brug *et al.*, "The analysis of electrode impedances complicated by the presence of a constant phase element," *J Electroanal Chem Interfacial Electrochem* vol. 176, no. 1, pp. 275–295, Sep. 1984.

[28] P. Zoltowski, "On the electrical capacitance of interfaces exhibiting constant phase element behaviour," *J. Electroanal. Chem.*, vol. 443, no. 1, pp. 149–154, Feb. 1998.

[29] H. Morgan and N. G. Green, *AC Electrokinetics: Colloids and Nanoparticles*. Research Studies Press, 2003.

[30] M. R. Shoar Abouzari *et al.*, "On the physical interpretation of constant phase elements," *Solid State Ion.*, vol. 180, no. 14, pp. 922–927, Jun. 2009.

[31] IEEE, "IEEE Standard for Digitizing Waveform Recorders, IEEE Standard 1057–2007." 2007.

[32] E. Ravagli and S. Severi, "Optical and Electrical Characterization of Biocompatible Polymeric Lines for Hemodialysis Applications," *Materials*, vol. 11, no. 3, p. 438, Mar. 2018.

[33] S. Rush, J. A. Abildskov, and R. McFee, "Resistivity of body tissues at low frequencies," *Circ. Res.*, vol. 12, pp. 40–50, Jan. 1963.

[34] L. A. Geddes and L. E. Baker, "The specific resistance of biological material--a compendium of data for the biomedical engineer and physiologist," *Med Biol Eng*, vol. 5, no. 3, pp. 271–293, May 1967.

[35] L. A. Geddes and H. Kidder, "Specific resistance of blood at body temperature II," *Med Biol Eng*, vol. 14, no. 2, pp. 180–185, Mar. 1976.
[36] E. D. Trautman and R. S. Newbower, "A practical analysis of the electrical conductivity of blood," *IEEE Trans Biomed Eng*, vol. 30, no. 3, pp. 141–154, Mar. 1983.
[37] K. R. Visser, "Electric conductivity of stationary and flowing human blood at low frequencies," *Med Biol Eng Comput*, vol. 30, no. 6, pp. 636–640, Nov. 1992.
[38] M. Wolf *et al.*, "Broadband dielectric spectroscopy on human blood," *Biochim. Biophys. Acta*, vol. 1810, no. 8, pp. 727–740, Aug. 2011.
[39] S. Abdalla, "Low frequency dielectric properties of human blood," *IEEE Trans Nanobioscience*, vol. 10, no. 2, pp. 113–120, Jun. 2011.
[40] C. Gabriel, S. Gabriel, and E. Corthout, "The dielectric properties of biological tissues: I. Literature survey," *Phys Med Biol*, vol. 41, no. 11, pp. 2231–2249, Nov. 1996.
[41] M. Jaggernath, *et al.*, "Diagnostic Accuracy of the HemoCue Hb 301, STAT-Site MHgb and URIT-12 Point-of-Care Hemoglobin Meters in a Central Laboratory and a Community Based Clinic in Durban, South Africa". *PLoS One*., Vol. 11, no. 4, 2016.
[42] J. B. Zhang, J. Lin, and X. D. Zhao, "Analysis of Bias in Measurements of Potassium, Sodium and Hemoglobin by an Emergency Department-Based Blood Gas Analyzer Relative to Hospital Laboratory Autoanalyzer Results," *PLoS One*., vol. 10, no. 4, p. e0122383, Apr. 2015.
[43] L. Chevalier *et al.*, "Isonatric Dialysis Biofeedback in Hemodiafiltration with Online Regeneration of Ultrafiltrate in Hypertensive Hemodialysis Patients: A Randomized Controlled Study," *Blood Purif*, vol. 41, no. 1–3, pp. 87–93, 2016.

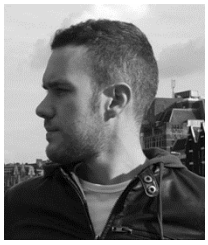

Enrico Ravagli received the B.Sc. and M.Sc. degrees in biomedical engineering from the University of Bologna, Italy, in 2010 and 2013, respectively. In 2017 he completed his PhD in Bioengineering at the same university with a thesis on non-invasive sensing and estimation methods for hemodialysis and extracorporeal circulation applications. He is currently a Research Associate at the Department of Medical Physics and Biomedical Engineering of University College London.

Marco Crescentini received the Dr.Eng degree (cum laude) in electronic engineering and the Ph.D degree in ICT from the University of Bologna, Italy, in 2008 and 2012, respectively. In 2009 he was an intern at Infineon Technologies, Villach, Austria, working on performance analysis of DC-DC converters. Since 2016, he has been Assistant Professor of Instrumentation and Measurement at the Department of Electrical, Electronic and Information Engineering "Guglielmo Marconi," Cesena Campus, University of Bologna. His research interests are in the design of high-accuracy, low-noise, and broadband instrumentation for either biomedical or industrial applications. He has co-authored more than 30 peer-reviewed journal/conference technical papers. Dr. Crescentini is a member of the Italian Association of Electrical and Electronic Measurement.

Paolo Rovatti received the Master's degree in Biomedical Engineering from the University of Bologna in 1989. He's currently at Baxter as Sr Manager for Renal Care Innovation area, having the main task to support and coordinate exploratory projects within the space of extracorporeal circulation devices and therapies.

Stefano Severi received the M.Sc. degree in Electronic Engineering and the PhD degree in Bioengineering from the University of Bologna, Italy. Assistant Professor at the Department of Electrical, Electronic and Information Engineering, University of Bologna. Head of the Computational Physiopathology Unit, with research focusing on computational cardiology, in silico pharmacology, artificial kidney and hemodialysis therapy.